Appraisal of (U-Th)/He apatite thermochronology as a thermal history tool for hydrocarbon exploration: An example from the Taranaki Basin, New Zealand

P. V. Crowhurst, P. F. Green, and P. J. J. Kamp

ABSTRACT

The Taranaki Basin contains most of New Zealand's commercial hydrocarbon reserves. The southern parts of the Taranaki Basin underwent inversion during the late Miocene, with published AFTA (apatite fission-track analysis) and vitrinite reflectance data suggesting approximately 2.5–3 km of section eroded from the structure on which the Fresne-1 well was drilled, consistent with estimates from reconstructions based on seismic sections. The well-constrained tectonic and thermal history framework for this well section, established by earlier studies, provides an ideal test bed for the thermochronological technique of apatite (U-Th)/He dating. Helium ages determined in apatites from the earlier AFTA study decrease from about 6 Ma at about 400 m depth to about 1 Ma at 2465 m. Although these results are qualitatively consistent with late Miocene cooling, quantitative modeling of (U-Th)/He ages based on best-fit thermal histories derived from new AFTA analyses (using improved methods) suggests that cooling was protracted, involving accelerated cooling during the Pliocene, possibly indicating a discrete Pliocene inversion phase. Integration of AFTA and (U-Th)/He dating can provide improved thermal history constraints in sedimentary basins, particularly on cooling rates and/or resolution of multiple thermal events. By independently defining the timing of peak maturation in relation to formation of potential trapping structures, this information offers the potential for improved assessment of hydrocarbon prospectivity and reduced exploration risk.

Manuscript received May 23, 2001; revised manuscript received April 29, 2002; final acceptance May 23, 2002.

AUTHORS

P. V. Crowhurst ~ *CSIRO Petroleum Resources, P.O. Box 136, North Ryde, New South Wales, 1670, Australia; peter.crowhurst@csiro.au*

Peter Crowhurst works at CSIRO Petroleum in Sydney on development of the (U-Th)/He thermochronology technique. Peter graduated with a B.Sc. (hons.) degree from Adelaide University, Australia, an M.Sc. degree at Monash University, Australia, and a Ph.D. project at La Trobe University, Australia, which involved redefining the tectonic history of northern Papua New Guinea. He also worked in the mineral exploration industry, mainly for BHP Minerals in Australia and Papua New Guinea.

P. F. Green ~ *Geotrack International Pty. Ltd., 37 Melville Rd., Brunswick West, Victoria, 3055, Australia; mail@geotrack.com.au*

Paul Green is technical director of Geotrack International, a private company specializing in thermal history reconstruction in sedimentary basins and its application to hydrocarbon exploration. He has a Ph.D. from the University of Birmingham, Great Britain, and has held research positions at the University of Birmingham, the University of Melbourne, Australia, and University College London. He is the author of more than 100 published papers on fission-track analysis and related topics and is a member of AAPG, the Petroleum Exploration Society of Australia, and the Petroleum Exploration Society of Great Britain.

P. J. J. Kamp ~ *Department of Earth Sciences, The University of Waikato, Private Bag 3105, Hamilton, New Zealand; p.kamp@waikato.ac.nz*

Peter Kamp is professor of earth sciences at the University of Waikato in Hamilton, New Zealand. His research interests are in the analysis of sedimentary basins, particularly those of Late Cretaceous–Cenozoic age in New Zealand. Another major research interest involves the techniques of fission-track analysis and (U-Th)/He thermochronometry. His research applications involve the thermal history of sedimentary basins and the exhumation history of basement provinces–mountain belts.

ACKNOWLEDGEMENTS

We thank Ken Farley of the California Institute of Technology for providing software for modeling helium diffusion and the (U-Th)/He age system in apatite. AFTA is the registered trademark of Geotrack International. P. J. J. Kamp acknowledges research funding from the New Zealand Foundation for Research, Science and Technology.

INTRODUCTION

The novel technique of (U-Th)/He dating of apatite is emerging as an important low-temperature thermochronometer that can be applied to many geological settings. In this article, we investigate the potential application of the technique as a tool for petroleum exploration in sedimentary basins, based on a case study from the Taranaki Basin in New Zealand. A well-constrained tectonic and thermal history framework for this region established by earlier studies provides an ideal test for the method.

Helium is produced within apatite grains as a result of alpha decay from uranium and thorium isotopes, which are present as impurities at parts per million levels. As reviewed by Lippolt et al. (1994), this process formed the basis of the first attempts at geochronology (Rutherford, 1907a). However, it soon became clear (e.g., Rutherford, 1907b) that at least a fraction of radiogenic helium was lost from the host crystal lattice, and with the advent of apparently more reliable methods of geochronology (e.g., K-Ar, Rb-Sr, U-Pb), interest in the helium systematics of minerals waned.

More recently, however, the realization that the partial loss of radiogenic products could provide quantitative information on the thermal history of mineral grains has led to a resurgence of interest in this topic (e.g., Zeitler et al., 1987; Lippolt et al., 1994). In particular, efforts at the California Institute of Technology through the 1990s led to the development of (U-Th)/He dating of apatite as a rigorous, quantitative technique (Wolf et al., 1996). Studies of the diffusion systematics of helium in apatite (Wolf et al., 1998; Farley, 2000) also revealed the unique temperature sensitivity of the technique, with all helium being lost over geological periods at temperatures as low as 90°C or less, and a closure temperature as low as 75°C. Several subsequent applications of the method (e.g., House et al., 1997; Warnock et al., 1997; Wolf et al., 1997) have illustrated the potential of the technique to provide useful thermochronometric information at temperatures in the 40–80°C range.

In principle, therefore, (U-Th)/He dating of apatite can be used to determine thermal histories in samples from depths of up to 2 km or more in sedimentary basins. This should provide a useful complement to the information provided by apatite fission-track analysis (AFTA), typically at paleotemperatures up to 110°C or more (e.g., Green et al., 1995). In this article, we assess this possibility in detail by considering (U-Th)/He ages in apatites from a hydrocarbon exploration well (well Fresne-1 in the Taranaki Basin of New Zealand) in the context of a thermal history framework defined by AFTA and vitrinite reflectance (R_o) data. Quantitative modeling of the (U-Th)/He ages, using the thermal history framework provided by AFTA and R_o data, is used to assess the consistency of the different techniques. Recent investigations of (U-Th)/He ages in samples from hydrocarbon exploration boreholes in the Otway Basin of southeastern Australia (House et al., 1999, 2002) suggest that helium diffusion systematics derived from laboratory

measurements can be extrapolated to geological conditions with confidence. The well-constrained thermal history framework provided by the AFTA and R_o data in the Fresne-1 well therefore provides an ideal test for this new application of apatite (U-Th)/He thermochronometry.

REGIONAL GEOLOGY

The Taranaki Basin lies along the western margin of North Island, New Zealand, mainly offshore beneath the modern continental shelf and slope (Figure 1). The basin has a composite morphology reflecting a middle Cretaceous–Holocene evolution in a variety of tectonic regimes (King and Thrasher, 1996). The early basin history (middle Cretaceous–Paleocene) was dominated by extensional tectonics with locally rapid, fault-controlled subsidence. Eocene–Oligocene development was characterized by postdrift thermal contraction and regional subsidence. During the Neogene, the eastern and southern parts of the basin become involved in the Australia-Pacific plate boundary zone through New Zealand, whereas other parts (Western Stable platform) have been more akin to a passive margin. Most of the structure at the margins and within the Taranaki Basin formed during the Neogene. Inversion structures developed mainly in the southern part of the basin, parallel with the Taranaki fault and including the Tarata thrust zone (Figure 1).

Several discrete anticlines form positive inversion structures. These originated through late Miocene reverse displacement on older existing normal faults that resulted in the inversion of Late Cretaceous–Eocene half grabens (Figures 1, 2). Many of these structures plunge to the north, rising to the south where they emerge onshore. Many of these inversion structures have been successfully tested for hydrocarbons. The Maui, Kapuni, and Kupe structures are good examples. The inversion was accompanied by erosion represented by an angular unconformity that truncates all of the structures and is a general feature in the southern inversion zone (King and Thrasher, 1996). The unconformity is flat, lying in the east-west direction, and rises to the south. It is onlapped in a southward direction by loosely constrained late Pliocene and Pleistocene sedimentary rocks, 100–200 m thick, that reflect recent submergence of the southern part of the Taranaki Basin.

The Cook and Wakamarama anticlines are prominent structures tested by the Cook-1 and Fresne-1 wells (Figures 1, 2), and they have been described and interpreted by Knox (1982), Kamp and Green (1990), King et al. (1991), Green et al. (1995), and Bishop and Buchanan (1995). The Fresne-1 well was drilled near the crest of the Wakamarama Anticline. It encountered the thick, Late Cretaceous Pakawau Group (923–2504 m depth), which accumulated as terrestrial deposits in a half graben bounded immediately to the east by the Wakamarama fault (Figure 1). This is overlain by the Kapuni Group (408–923 m depth), which also accumulated in terrestrial environments, with continuing displacement on the Wakamarama fault but with a more even thickness distribution in the basin. An Eocene–early Oligocene unconformity separates the Kapuni Group from overlying, thin, upper Oligocene to lower–middle Miocene calcareous to muddy strata (203–408 m depth). Above another unconformity is a 120 m–thick section between seabed (83 m) and 203 m depth that is poorly dated but, based on regional correlation, is of late Pliocene–Pleistocene age.

The inversion of the Wakamarama and Cook anticlines postdates the middle Miocene, based on the presence of lower–middle Miocene beds preserved on the flanks of these structures. Inversion of both anticlines probably occurred at the same time. The bounding faults are antithetic such that the two half grabens and intervening strata form a pop-up structure (Figure 2). In both anticlines the crest is formed above the thickest synrift sequence. In the Wakamarama Anticline the upper Eocene horizon is displaced about 2.5 km on the fault, but at basement level the sense of throw remains normal, reflecting a greater amount of Late Cretaceous extension compared with late Neogene compression.

Several estimates have been made of the thickness of section eroded at the middle Miocene–late Pliocene unconformity in the Fresne-1 well. Based on seismic reflection data, Knox (1982) estimated greater than 2.0 km of removed section, Ellyard and Beattie (1990) 3.5 km, King et al. (1991) greater than or equal to 2.8 km, and Bishop and Buchanan (1995) about 3.0 km. Based on AFTA, Kamp and Green (1990) estimated 3.0 ± 0.3 km of missing section, and from offset in porosity vs. depth trends (Funnell et al., 1996; Armstrong et al., 1998), they estimated 3.0 km of eroded section. The only numerical ages on the timing of erosion have been established from AFTA (Kamp and Green, 1990) at between 12 and 8 Ma. The poorly dated upper Pliocene–Pleistocene deposits overlying the Wakamarama Anticline currently provide the only constraints on the timing of the end of erosion.

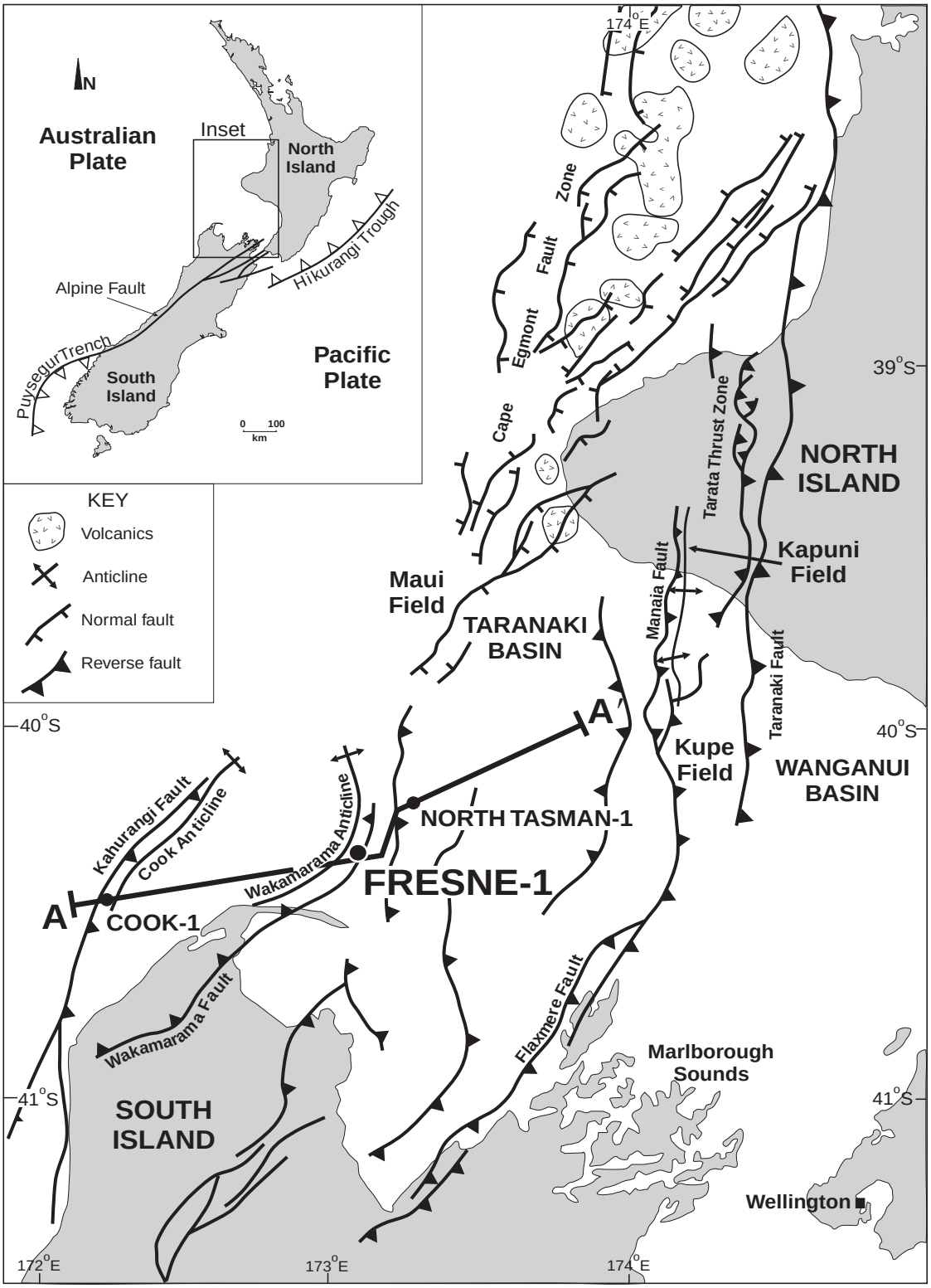

Figure 1. Map of central-western New Zealand showing the location of the Taranaki Basin (west of the Taranaki fault and north of South Island) and some of the main oil and gas fields. Also shown are the location of the Fresne-1 drill hole and the line of cross section AA′ illustrated in Figure 2.

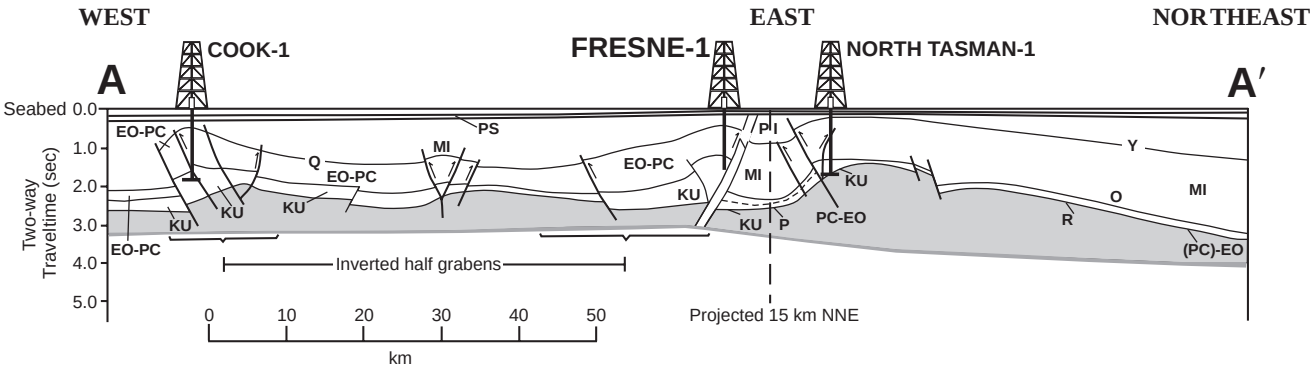

Figure 2. Cross section (see line on Figure 1) through the southern inversion zone of the Taranaki Basin showing the inversion structures penetrated by the Fresne-1, Cook-1, and North Tasman-1 wells. PS = Pleistocene; PI = Pliocene; MI = Miocene; EO = Eocene; PC = Paleocene; KU = Upper Cretaceous; Y = near base Pliocene horizon; Q = near base Oligocene horizon; P = near top Cretaceous horizon; R = top basement seismic horizon.

THERMAL HISTORY RECONSTRUCTION USING APATITE FISSION-TRACK ANALYSIS AND VITRINITE REFLECTANCE

To construct a thermal history framework within which the (U-Th)/He ages can be understood, we have used thermal history reconstruction based on application of AFTA and R_o data. Using this approach, it is possible to identify the timing of dominant episodes of heating and cooling that have affected a sedimentary section, quantify the paleotemperature through the section, and characterize mechanisms of heating and cooling (e.g., Bray et al., 1992; Duddy et al., 1994; and Green et al., 1995). This information allows the thermal history of all units within the sedimentary section to be reconstructed within a framework constrained by measured data.

For details on the thermal history response of fission tracks in apatite, the development of AFTA parameters, and the use of AFTA and R_o to extract thermal history solutions in sedimentary basins, see Green et al. (in press).

Thermal History Interpretation of AFTA and R_o Data

Extraction of thermal history solutions from AFTA and R_o data is based on detailed knowledge of the kinetic responses of both systems, which are calibrated from studies in both geological and laboratory conditions. Thermal history information is extracted from AFTA data by modeling the AFTA parameters (fission-track age and track-length distributions) expected from a variety of possible thermal history scenarios and comparing these with the measured data. By varying the magnitude and timing of the maximum paleotemperature employed in the modeling, the range of values of these parameters, which give predictions consistent with the measured data within 95% confidence limits, can be rigorously defined.

The basics of this modeling procedure are well established for monocompositional apatites (e.g., Green et al., 1989), based on a series of laboratory experiments on Durango apatite (Green et al., 1986; Laslett et al., 1987; Duddy et al., 1988). However, the annealing kinetics of fission tracks in apatite is known to be affected by the chlorine content (Green et al., 1986). In the studies described in this article, thermal history solutions have been extracted from the AFTA data using a multicompositional kinetic model, which makes full quantitative allowance for the effect of chlorine content on annealing rates of fission tracks in apatite (Green et al., 1996). This model is calibrated using a combination of laboratory and geological data from a variety of sedimentary basins around the world. Paleotemperature estimates from AFTA are quoted as a range (corresponding to ±95% confidence limits) and have an absolute uncertainty between ±5 and ±10°C.

Observed R_o values are converted to maximum paleotemperature using the kinetic model developed by Burnham and Sweeney (1989) and Sweeney and Burnham (1990). Information on the timing of these maximum paleotemperatures is provided by the AFTA data. The R_o-derived paleotemperature estimates are shown as single values but have a precision between 5 and 10°C. The kinetic response of R_o as described by Burnham and Sweeney (1989) is very similar to the fission-track annealing kinetic model developed by

Laslett et al. (1987) to describe the kinetics of fission-track annealing in Durango apatite. Total fission-track annealing in apatites with typical chlorine content corresponds to an R_o value of about 0.7%, regardless of heating rate (Duddy et al., 1991, 1994).

As explained in more detail by Green et al. (in press), both AFTA and R_o are dominated by the maximum paleotemperature reached by a sample and preserve no information on the history prior to the onset of cooling from that maximum. Therefore, to interpret the data, it is necessary to assume a value of heating rate, and the precise value of maximum paleotemperature required to explain the data depends on the assumed value of heating rate. An order of magnitude change in the heating rate is equivalent to a change of about 10°C in the required paleotemperature (Green et al., 1989).

New AFTA Data from Fresne-1

The AFTA data from the Fresne-1 well were first reported by Kamp and Green (1990), who obtained thermal history interpretations using a monocompositional kinetic model (Laslett et al., 1987). The multicompositional model used in our study incorporates the effects of variation in kinetic response between apatites of different composition (chlorine content) and provides more accurate definition of both the magnitude and timing of maximum paleotemperatures from AFTA data (Green et al., 1996, in press). The new model also provides an improved description of low-temperature response compared to the Laslett et al. (1987) model, which is known to produce anomalous late-stage cooling as an artifact of the model (Green et al., in press). Samples originally analyzed by Kamp and Green (1990) have been reanalyzed, using latest methods that include measurement of chlorine contents in every apatite grain analyzed. Chlorine contents were measured using an automated electron microprobe, which derives apatite grain locations from the computer-controlled microscope system used for fission-track analysis.

The new fission-track ages (Table 1) are generally very similar to those reported by Kamp and Green (1990), showing a progressive reduction from values around 80 Ma in the shallowest part of the Upper Cretaceous–lower Tertiary coal measures section to values consistently around 5–10 Ma at depths greater than 1500 m (Figure 3). As discussed by Kamp and Green (1990), this pattern is characteristic of sections that have been hotter in the past. The depth marking the

Table 1. Sample Details and AFTA Data for Samples from the Fresne-1 Well, Taranaki Basin, New Zealand

Sample Number	Depth (m rkb)	Stratigraphic Age* (Ma)	ρ_s** (10^6 tracks/cm^2)	ρ_i†† (10^6 tracks/cm^2)	Pooled/Central Fission-Track Age†† (Ma)	$P(\chi^2)$ (%)	Number of Grains	Mean Track Length (μm)	Standard Deviation (Number of Lengths)
8694-7	419–446	53	1.007 (959)	2.960 (2820)	77.0 ± 3.5	14.3	25	11.15 ± 0.15	1.70 (132)
8	689–722	59	0.639 (621)	2.188 (2126)	64.9 ± 4.8	<1	30	11.27 ± 0.18	2.04 (133)
9	1049–1067	66	0.523 (866)	3.306 (5472)	28.6 ± 4.5	<1	36	10.60 ± 0.29	2.95 (12)
10	1319–1346	68	0.202 (316)	1.818 (2841)	22.0 ± 4.6	<1	32	11.43 ± 0.41	3.30 (64)
11	1620–1650	70	0.130 (210)	2.077 (3367)	13.3 ± 2.9	<1	30	12.03 ± 0.27	2.21 (66)
12	1889–1913	72	0.040 (63)	1.688 (2674)	5.5 ± 0.9	<1	34	13.10 ± 0.35	1.44 (17)
13	2189–2225	75	0.032 (51)	1.529 (2409)	4.9 ± 0.7	37	34	13.21 ± 0.32	1.45 (21)
14	2450–2480	77	0.058 (83)	1.693 (2433)	8.5 ± 2.4	<1	34	12.05 ± 0.55	1.83 (11)

*From Kamp and Green (1990).
**ρ_s = spontaneous track density. Numbers in parentheses show the number of tracks counted.
†ρ_i = induced track density. Numbers in parentheses show the number of tracks counted.
††Central age (Galbraith and Laslett, 1993) is used for samples containing a significant spread in single grain ages ($P(\chi^2) < 5\%$), otherwise the pooled age is shown. Other details are as described by Kamp and Green (1990). All ages were calculated using the zeta calibration approach of Hurford and Green (1983), using a value of 1.292 x 10^6 tracks/cm^2 for ρD (track density in mica detector adjacent to standard reference glass) and a zeta of 353.5 ± 3.9 (Green, 1985). All errors quoted at $\pm 1\sigma$.

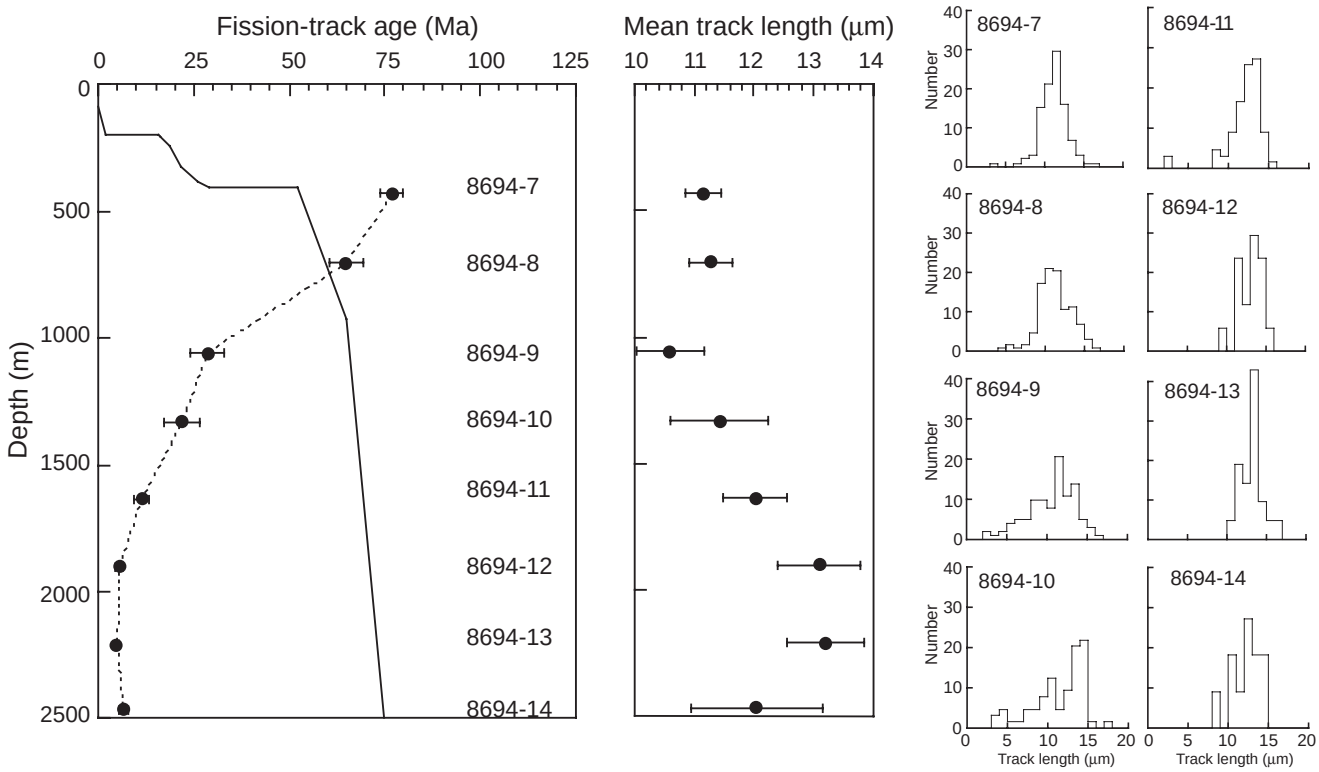

Figure 3. Pooled or central fission-track ages and mean confined track lengths in samples from the Fresne-1 well (all values summarized in Table 1) plotted against depth. Distributions of confined track lengths are also shown for each sample. These new results are very similar to values originally reported by Kamp and Green (1990).

transition from rapidly decreasing ages to consistent values at greater depths corresponds to a paleotemperature at which all samples were totally annealed prior to the onset of cooling (taken to be 130°C by Kamp and Green [1990], reflecting the rapid time scale of heating and cooling).

Track-length data (Figure 3; Table 1) show a sympathetic trend to that of the age data, with shallower samples giving short mean lengths and broad distributions, whereas deeper samples give longer mean lengths and the long mode of the distribution becomes dominant. These length distributions represent the combined effects of shorter tracks formed prior to cooling and longer tracks formed after cooling began. The changing trends with depth reflect progressive length reduction of the population of tracks formed prior to the onset of cooling, which are totally annealed in the four deepest samples, leaving only the longer tracks formed after the onset of cooling.

The variation of fission-track age with chlorine content for individual apatite grains within each sample (Figure 4) provides further thermal history information. In samples 8694-7 and 8694-8 (Figure 4a, b), in which the central or pooled fission-track ages are greater than the stratigraphic age of the samples (implying only minor or moderate annealing), the individual grain ages show little or no variation with chlorine content. In contrast, single-grain fission-track ages in sample 8694-9 (Figure 4c), in which the central fission-track age is reduced to less than 50% of the stratigraphic age (implying severe annealing), show a very different trend. Grains containing less than 0.1 wt. % chlorine have very young ages, but ages increase with chlorine content such that grains with greater than 0.3 wt. % chlorine give fission-track ages that are indistinguishable from the stratigraphic age. Results from deeper samples show similar effects, but the transition from very young ages to much older ages occurs at progressively higher chlorine contents as depth increases. In the deepest sample, 8694-14 (Figure 4h), all grains except for that with the highest chlorine content, between 0.6 and 0.7 wt. % chlorine (plus an apparent outlier containing between 0.3 and 0.4 wt. % chlorine), give very young ages.

The trends of the data in Figure 4 illustrate the influence of chlorine content on the annealing

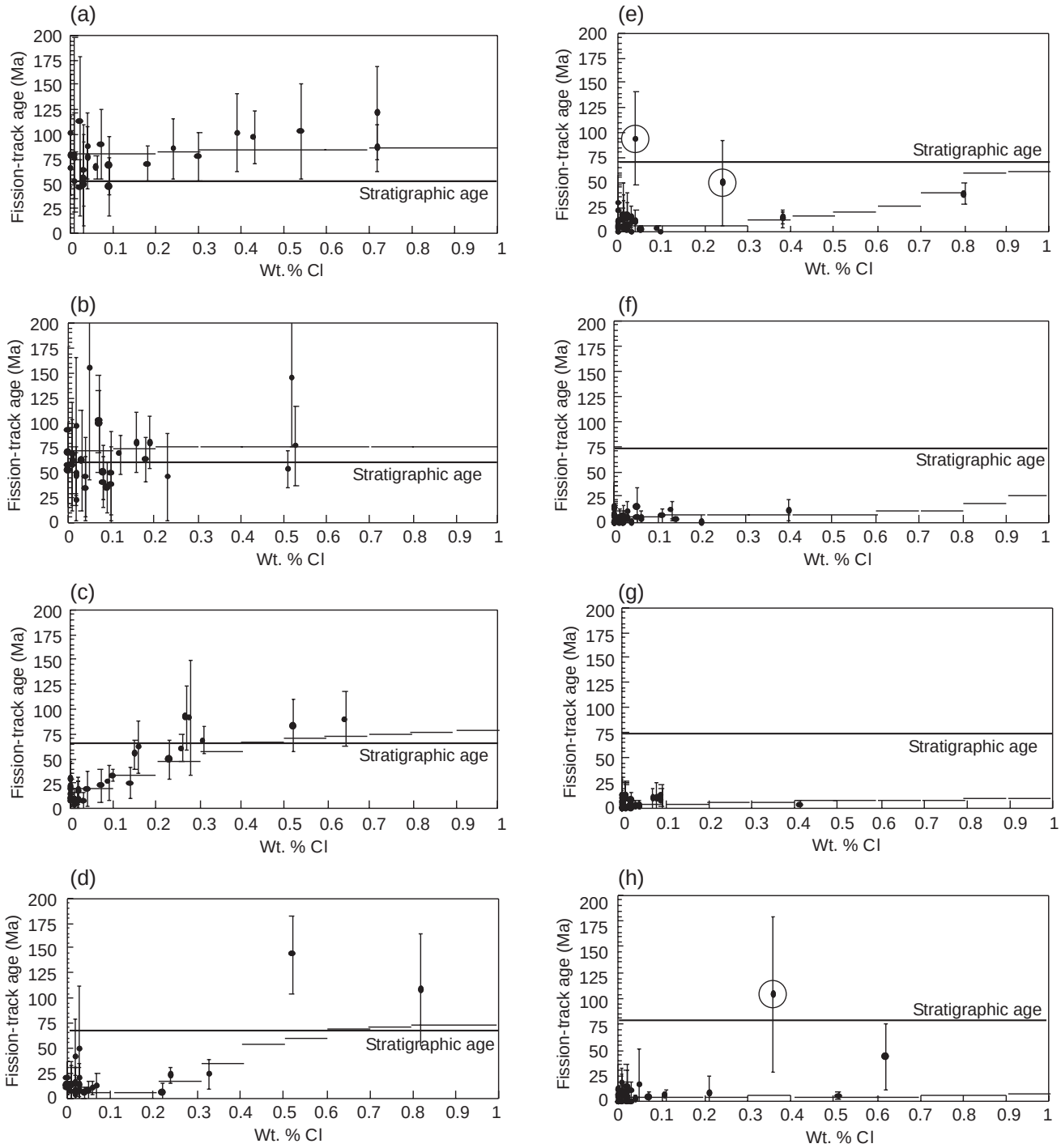

Figure 4. Fission-track ages of individual apatite grains in samples from the Fresne-1 well plotted against the chlorine content of each grain (chlorine contents were measured using an electron microprobe). These results illustrate the influence of chlorine content on fission-track annealing rates, as discussed in the text. Horizontal lines show the trend of age vs. chlorine content in each sample predicted by the best-fit thermal history solutions derived from these data. A few grains (circled) do not fall within this overall pattern, highlighting possible secondary controls on annealing rates, which are, as yet, undefined. (a) Sample 8694-7, 22°C; (b) sample 8694-8, 29°C; (c) sample 8694-9, 39°C; (d) sample 8694-10, 47°C; (e) sample 8694-11, 55°C; (f) sample 8694-12, 63°C; (g) sample 8694-13, 72°C; (h) sample 8694-14, 79°C.

sensitivity of fission tracks in apatite. With increasing present-day depth in the well, the fission-track ages of the samples are progressively reduced, as shown in Figure 3, corresponding to increasing maximum paleotemperatures prior to the onset of cooling. The rate of fission-track annealing (age and length reduction), however, depends critically on the chlorine content and is more rapid in apatites with little or no chlorine compared to those with higher chlorine contents. Therefore, within each sample, apatites with different chlorine contents reached different degrees of age and length reduction at the time of maximum paleotemperatures. In the deeper samples, lower chlorine content grains were totally annealed prior to the onset of cooling, whereas higher chlorine content grains were only partially reset. The totally reset fission-track ages provide the best constraint on the time of cooling. The range of chlorine contents of those apatites, which were totally annealed prior to the onset of cooling (i.e., those giving very young ages), increases with depth, so that only the highest chlorine contents are not totally annealed in the deepest samples.

Results from a few grains, circled in Figure 4, do not fit within the general pattern. These results suggest that secondary controls on annealing rates exist in addition to the first-order control exerted by chlorine content. Data from these grains have been removed prior to detailed thermal history interpretation.

Figure 5 further highlights the importance of compositional effects in these data, illustrating how fission-track ages of lower chlorine content apatites become totally annealed at lower maximum paleotemperatures (i.e., at shallower depths) compared to those required to totally anneal the higher chlorine content apatites.

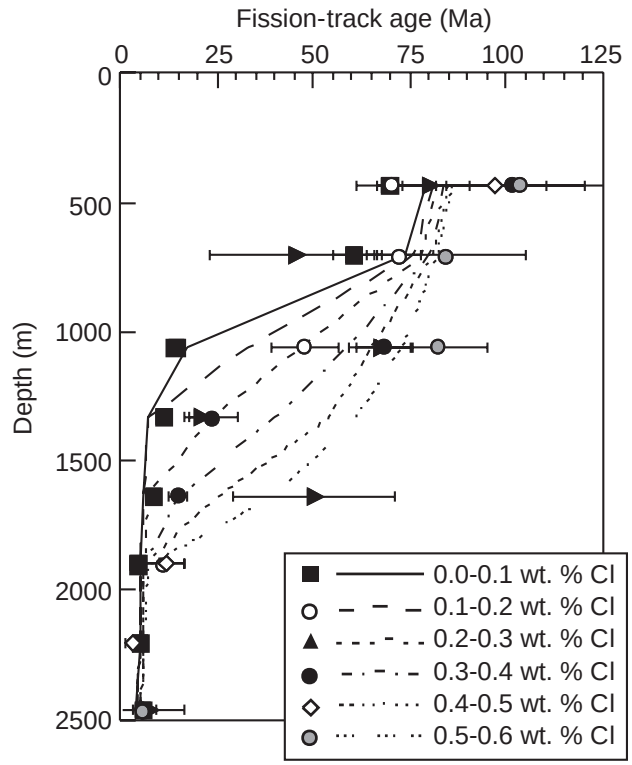

Figure 5. Pooled or central fission-track ages for discrete compositional groups within samples from Fresne-1 plotted against depth. The behavior of the data in this plot is more erratic than that in Figure 3, due mainly to the small numbers of grains involved in each data point. However, the trend is clear, with apatites with higher chlorine contents achieving a particular degree of age reduction at progressively deeper levels, corresponding to higher maximum paleotemperatures. This is emphasized by the curves, which show the variation of fission-track age with depth for different chlorine contents predicted by the final reconstructed thermal histories of individual samples (corresponding to the horizontal lines in Figure 4).

Thermal History Interpretation of AFTA and R_o Data from the Fresne-1 Well

Using the procedure outlined in a preceding section, thermal history solutions have been derived from the AFTA data in the eight samples from the Fresne-1 well. Note that we do not attempt to constrain the whole thermal history of each sample. Instead, we focus on those aspects of the thermal history that control the development of the AFTA parameters, specifically the maximum paleotemperature of each sample and the time at which cooling from that paleotemperature began. Estimates of these parameters are presented for each sample in Table 2, as ranges of allowed values, corresponding to $\pm 95\%$ confidence intervals. These are defined by comparing measured data with values predicted from a range of likely thermal history scenarios. By systematically varying the timing of the onset of cooling and the peak paleotemperature, rigorous statistical procedures are used to formally define the range of conditions for which the modeled parameters are compatible with the measured data (within analytical uncertainties). Estimates of maximum paleotemperature derived from R_o data (discussed by Kamp and Green [1990] and originally taken from Lowery [1988]) are also shown in Table 2.

These results are based on assumed heating and cooling rates of 10°C/m.y. Unlike R_o data, which only provide a value for the maximum paleotemperature, AFTA data commonly can provide some control on the history after cooling from maximum

Table 2. Thermal History Interpretation of AFTA and R_o Data from the Fresne-1 Well, Taranaki Basin, New Zealand

Sample Number	Depth (m rkb)	Stratigraphic Age* (Ma)	Maximum Paleotemperature from AFTA (°C)	Onset of Cooling from AFTA (Ma)	Mean R_o** (%)	Maximum Paleotemperature from R_o†
8694-7	419–446	53	95–105	13–3		
	701				0.54 ± 0.04	100
8694-8	689–722	59	100–110	20–8		
	1040				0.59 ± 0.02	107
8694-9	1049–1067	66	110–120	14–6		
	1280				0.64 ± 0.03	116
8694-10	1319–1346	68	105–120	16–8		
	1523				0.62 ± 0.03	112
8694-11	1620–1650	70	110–125	14–8		
	1841				0.72 ± 0.03	129
8694-12	1889–1913	72	>120	10–5		
	2060				0.77 ± 0.06	135
8694-13	2189–2225	75	>140	9–8		
	2342				0.94 ± 0.09	150
	2462				0.82 ± 0.04	139
8694-14	2450–2480	77	>130	10–8		

*From Kamp and Green (1990).

**From Lowery (1988), taking data only from the PR1013 source on the basis that these are more reliable and provide a more coherent depth trend. All errors quoted at $\pm 1\sigma$.

†Calculated assuming a heating rate of 1°C/m.y. and a cooling rate of 10°C/m.y. Increasing or decreasing the heating rate by an order of magnitude is equivalent to an increase or decrease of ~10°C in the required maximum paleotemperature.

paleotemperature, from the lengths of tracks formed during this period. Thus, it is commonly possible to resolve two or, rarely, three discrete paleothermal episodes from AFTA data in a single sample. This is most straightforward when an earlier heating event causes significant age and length reduction, whereas a subsequent event produces only moderate length reduction. However, in samples from the Fresne-1 well, cooling from maximum paleotemperature began relatively late in the history (see the discussion in the next section). For this reason, apatite grains, which were not totally annealed prior to the onset of cooling, contain only a small proportion of tracks formed during the cooling history, whereas in samples that were totally annealed, the number of tracks present in the apatites is very low. Therefore, track-length data from the Fresne-1 well provide little or no information on the style of cooling. In thermal history interpretation of the new AFTA data from the Fresne-1 well, we have assumed simple, linear cooling. Available track-length data are consistent with this scenario.

Estimated times for the onset of cooling in the eight samples (Table 2) are all consistent with the interval 9 to 8 Ma, which represents the best available estimate of the time at which cooling began. This timing is consistent with the somewhat broader estimate of 12 to 8 Ma provided by Kamp and Green (1990). The improved precision highlights the advantages of the techniques employed in our study. The refined timing estimate also falls within the period represented by the late Miocene–Pliocene unconformity in the Fresne-1 well and is consistent with an interpretation of the observed paleothermal effects in terms of heating due to deeper burial and cooling related to subsequent late Miocene basin inversion.

Paleotemperature Profiles, Paleogeothermal Gradients, and Removed Section

Analysis of a series of samples using AFTA and R_o data over a range of depths reveals the variation of maximum paleotemperature with depth that characterizes a particular paleothermal episode. This paleotemperature profile provides key information on likely mechanisms of heating and cooling (e.g., Bray et al., 1992; Duddy et al., 1994; Green et al., 1995, in press). Heat-

ing due solely to deeper burial should produce a more or less linear paleotemperature profile with a similar gradient to the present temperature profile. In contrast, heating due primarily to increased basal heat flow (perhaps also with a minor component of deeper burial) should produce a more or less linear paleotemperature profile with a higher gradient than the present temperature profile. Nonlinear profiles are diagnostic of lateral introduction of heat, perhaps by hot fluid circulation, but are not relevant to results from the Fresne-1 well.

Estimates of maximum paleotemperature derived from AFTA and R_o data (Table 2) are highly consistent and define a linear depth profile (Figure 6). The slope is similar to that of the present-day temperature profile, suggesting that heating was due principally to deeper burial. This can be assessed quantitatively by fitting a line to the paleotemperature profile to obtain an estimate of the paleogeothermal gradient at the paleothermal maximum. Extrapolating the fitted linear profile to an assumed paleo–surface temperature provides an estimate of the amount of section removed by erosion. This analysis depends on several assumptions, as discussed in detail by Bray et al. (1992) and Green et al. (in press), but the consistency of the results with geological constraints (discussed elsewhere) suggests that the results are reliable. Statistical techniques can be used to define the range of each parameter allowed by the paleotemperature constraints within 95% confidence limits (Bray et al., 1992).

Application of these methods to the paleotemperature constraints from AFTA and R_o in the Fresne-1 well defines a maximum likelihood paleogeothermal gradient of 24.5°C/km, with upper and lower 95% confidence limits of 30 and 19°C/km, respectively (Figure 7). The present-day geothermal gradient of 28°C/km (Kamp and Green, 1990) falls within this range, and, given the relatively late timing for the main cooling phase, it is likely that the paleogeothermal gradient at the time at which cooling began was close to this value. (Funnell et al. [1996] estimated a present-day thermal gradient of 30°C/km for the Fresne-1 well, but the value of 28°C/km used by Kamp and Green [1990] was derived using methods that have proven consistent with AFTA and R_o data in a range of different settings and is preferred here.) From Figure 7, a paleogeothermal gradient of 28°C/km corresponds to between 2550 and 2800 m of removed section. Thus, we adopt the midpoint value of 2675 m as the best estimate of the amount of section removed on the late Miocene–Pliocene unconformity in the Fresne-1 well.

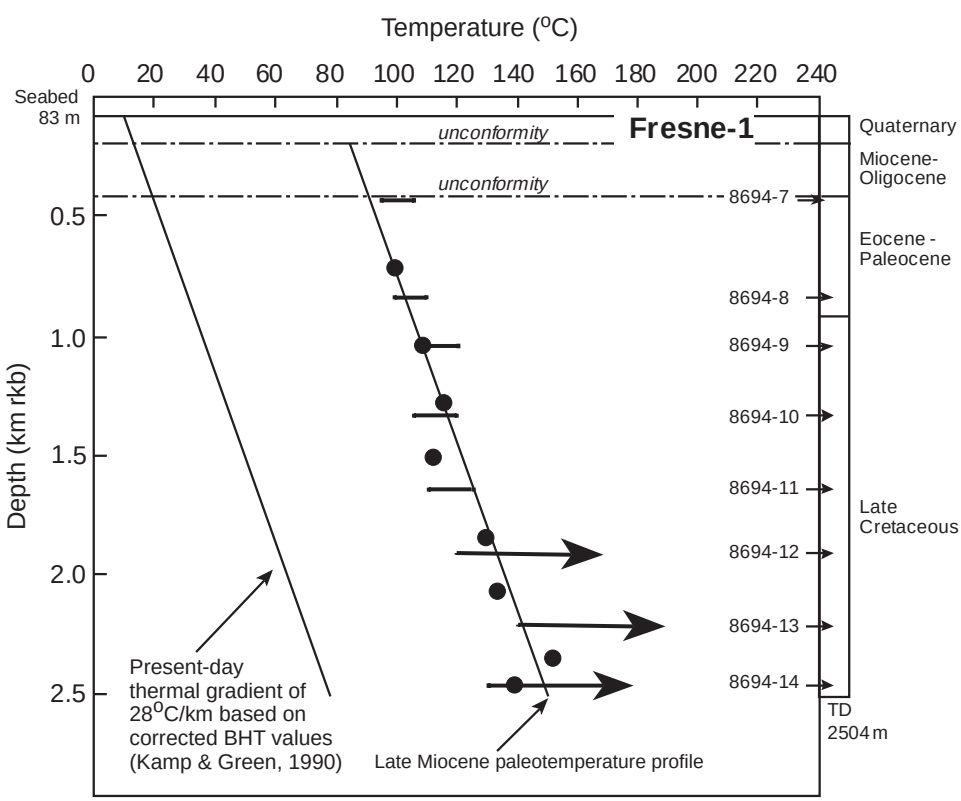

Figure 6. Late Miocene paleotemperatures from AFTA and R_o data in the Fresne-1 well (from Table 2) plotted against depth. These constraints can be used to constrain possible values of paleogeothermal gradient and removed section, as illustrated in Figure 7. BHT = bottom-hole temperature.

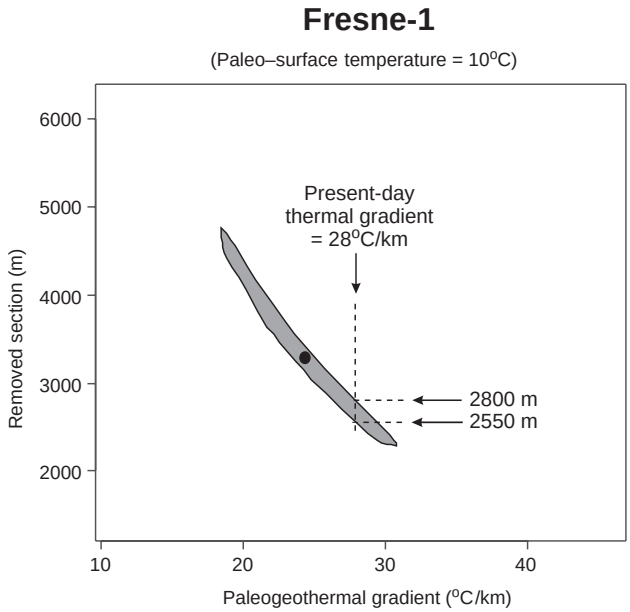

Figure 7. The shaded region shows the allowed ranges (within 95% confidence limits) of paleogeothermal gradient and removed section, which are consistent with the late Tertiary paleotemperature constraints from AFTA and R_o. Maximum likelihood estimates are represented by the black dot. The correlation in the allowed values of the two parameters results because the removed section estimates are obtained by extrapolation of fitted linear paleotemperature profiles (Bray et al., 1992), with higher gradients requiring lower amounts of removed section and vice versa. Assuming that the thermal gradient has been constant since 10 Ma, a paleogeothermal gradient equal to the present-day value of 28°C/km requires between 2550 and 2800 m of removed section on the late Miocene–Pliocene unconformity in Fresne-1.

Thermal History Synthesis

Taking values of 28°C/km for the paleogeothermal gradient and 2675 m of section removed, reconstructed thermal histories for units intersected in the Fresne-1 well are shown in Figure 8a. Although we have assumed here that heating was solely due to deeper burial, with no change in geothermal gradient (heat flow), alternative scenarios are possible, and a variety of combinations of paleogradient and removed section (shown by the shaded region in Figure 7) are capable of satisfying the paleotemperature constraints. However, all such combinations of paleogeothermal gradient and removed section result in reconstructed thermal histories for the preserved units that are very similar to those shown in Figure 8, being tightly constrained to meet the paleotemperature constraints defined by AFTA and R_o data throughout the well.

The late Miocene–Pliocene unconformity in the Fresne-1 well spans the interval 15.5 to 2 Ma (Kamp and Green, 1990), and the total amount of heating and cooling required by the AFTA and R_o data is about 75°C, and AFTA results show that cooling began at around 8.5 Ma. Thus the heating and cooling rates of 10°C/m.y. assumed in interpreting the data appear to be realistic. With the amount of removed section highly consistent with previous estimates ranging between 2 and 3.5 km based on geological constraints (see preceding discussion), all aspects of the thermal history reconstruction illustrated in Figure 8a for units intersected in the Fresne-1 well can be regarded as reliable.

APATITE (U-TH)/HE DATING RESULTS

Having established a basic thermal history framework for the Fresne-1 well, aliquots from the same apatite samples used for AFTA were analyzed using (U-Th)/He dating (Table 3) to investigate the consistency of such data with AFTA and R_o and to assess the suitability of this method for application to exploration settings. Where possible, at least two aliquots of a sample were analyzed to check reproducibility and to confirm the level of precision that can be obtained. On average, each aliquot contained approximately 18 grains, selected on the basis of euhedral form and clarity to ensure the absence of inclusions that can interfere with the analysis (see Appendix). The absence of a significant contribution to the analyses from inclusions is supported by the small number of reextracts during helium outgassing.

Considering the low ages in this suite of samples (Table 3), the reproducibility appears to be very good. Only sample 8694-9 showed a spread in ages between the three aliquots analyzed. Such a spread could arise from grain size variation between aliquots or from a minor amount of downhole sample contamination (Tables 3, 4). Because the results in Table 4 show only minor variation in the average grain sizes for the three aliquots of sample 8694-9, it is more likely due to contamination of the sample. An alternative explanation might be the presence of inclusions that totally outgassed but did not dissolve in nitric acid, thus yielding an older apparent age.

The (U-Th)/He ages are younger than the corresponding fission-track ages (Figure 9), consistent with the lower closure temperature for helium retention in apatite. In contrast to the fission-track ages, helium

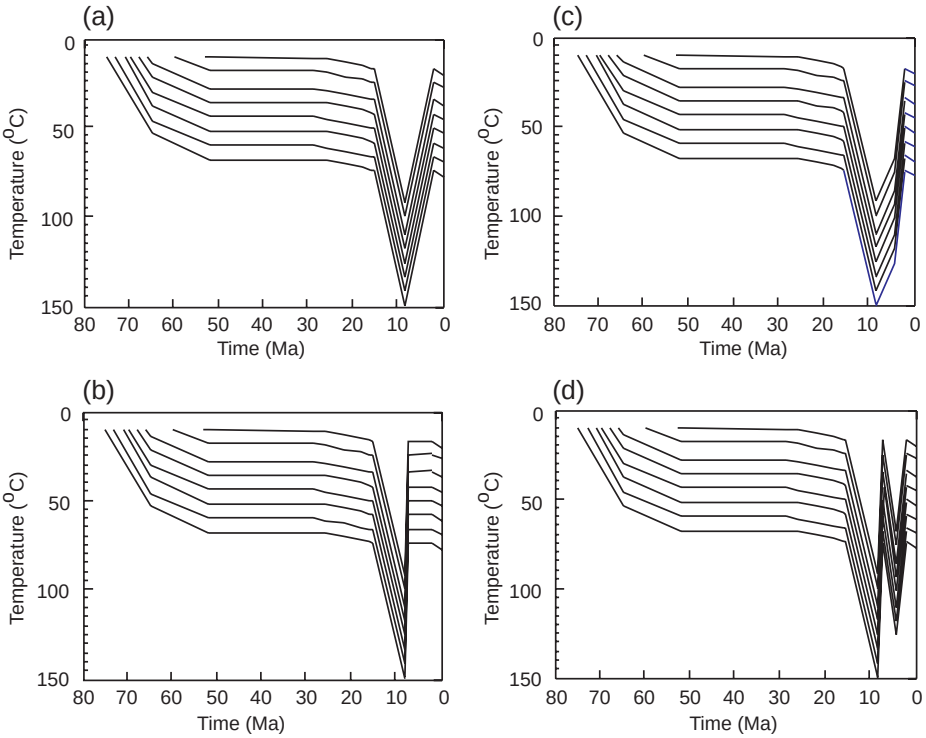

Figure 8. Reconstructed thermal histories for the eight AFTA samples from the Fresne-1 well based on the interpretation of AFTA and R_o data. All four scenarios are based on late Miocene heating due to burial by 2675 m of section, with a constant paleogeothermal gradient of 28°C/km, and cooling beginning at 8.5 Ma. Four different styles of cooling have been used to model (U-Th)/He ages: (a) linear heating and cooling; (b) rapid cooling; (c) protracted cooling; (d) two separate cooling events.

ages decrease only slowly with increasing depth. By analogy with the AFTA results, this suggests that helium was totally outgassed from all samples prior to the onset of cooling. Helium ages around 6 Ma in the shallowest samples are similar to fission-track ages in the deepest samples, consistent with late Miocene initiation of cooling as indicated by the interpretation of the AFTA data (Table 2). However, because of continuing helium loss at temperatures below the closure temperature during cooling, the helium ages do not

Table 3. (U-Th)/He Age Data from the Fresne-1 Well, Taranaki Basin, New Zealand

Sample ID	^{4}He (ncm^2)	Total U (atoms × 10^{12})	Total Th (atoms × 10^{12})	Th/U	U Content (ppm)	Th Content (ppm)	F_T*	Uncorrected (U-Th)/He Age (Ma)	Corrected (U-Th)/He Age (Ma)
8694-7b	0.177 ± 0.024	0.533 ± 0.008	1.540 ± 0.290	2.88	10.3	28.9	0.68	4.17	6.14 ± 0.64
7c	0.167 ± 0.020	0.484 ± 0.008	1.580 ± 0.301	3.26	7.6	24	0.64	4.12	6.44 ± 0.60
8a	0.164 ± 0.012	0.768 ± 0.013	1.290 ± 0.028	1.68	16.8	27.3	0.65	3.22	4.96 ± 0.24
8b	0.233 ± 0.017	0.819 ± 0.013	2.730 ± 0.051	3.33	8.4	27	0.72	3.37	4.68 ± 0.25
9a	0.614 ± 0.022	2.260 ± 0.039	4.460 ± 0.080	1.97	15.5	29.6	0.74	3.9	5.27 ± 0.15
9b	0.361 ± 0.015	1.650 ± 0.026	5.390 ± 0.095	3.27	5	15.8	0.76	2.61	3.44 ± 0.11
9c	0.481 ± 0.016	1.800 ± 0.027	6.090 ± 0.099	3.5	10	32.5	0.7	3.14	4.48 ± 0.11
10a	0.61 ± 0.021	3.800 ± 0.063	10.70 ± 0.168	2.83	7.8	21.4	0.8	2.03	2.54 ± 0.07
10b	0.394 ± 0.013	2.430 ± 0.037	6.420 ± 0.105	2.65	10.4	26.7	0.74	2.11	2.85 ± 0.07
11a	0.126 ± 0.032	1.160 ± 0.018	2.980 ± 0.056	2.58	9.5	23.7	0.73	1.43	1.96 ± 0.37
11b	0.115 ± 0.016	1.030 ± 0.017	2.210 ± 0.041	2.14	8.3	17.3	0.68	1.56	2.29 ± 0.22
12a	0.100 ± 0.021	1.000 ± 0.016	2.620 ± 0.045	2.61	10.7	25.8	0.67	1.3	1.95 ± 0.27
13b	0.125 ± 0.016	1.580 ± 0.025	4.720 ± 0.087	2.98	7.6	21.8	0.75	0.98	1.31 ± 0.13
13c	0.208 ± 0.020	2.700 ± 0.043	6.740 ± 0.110	2.49	10.5	25.3	0.75	1.02	1.36 ± 0.10
14a	0.078 ± 0.016	1.350 ± 0.026	3.470 ± 0.060	2.57	9.4	23.3	0.68	0.76	1.12 ± 0.15

*Size correction factor (Farley et al., 1996). All errors quoted at ±1σ.

Table 4. (U-Th)/He Age Data and Average Grain Sizes of Apatites from the Fresne-1 Well, Taranaki Basin, New Zealand

Sample Number	(U-Th)/He age (Ma)	Average Radius (μm)	Number of Grains	Standard Deviation (μm)
8694-7b	6.14 ± 0.64	41	8	6.3
8694-7c	6.44 ± 0.60	37.6	12	4.8
8694-8a	4.96 ± 0.24	38.5	10	5
8694-8b	4.68 ± 0.25	46	12	10.4
8694-9a	5.27 ± 0.15	50	14	10
8694-9b	3.44 ± 0.11	57	22	7.8
8694-9c	4.48 ± 0.11	48.9	19	9.9
8694-10a	2.54 ± 0.07	67.9	20	13.5
8694-10b	2.85 ± 0.07	50.4	22	10
8694-11a	1.96 ± 0.37	47.8	12	8.4
8694-11b	2.29 ± 0.22	41.7	20	7.2
8694-12a	1.95 ± 0.27	38.5	19	6.8
8694-13b	1.31 ± 0.13	54	16	10.2
8694-13c	1.36 ± 0.10	54.9	20	9.4
8694-14a	1.12 ± 0.15	41.6	22	5.8

represent the timing of any specific particular event in their own right. To completely understand these ages more completely, it is necessary to compare the measured data with results of modeling the (U-Th)/He system through a variety of scenarios to determine the range of thermal history solutions consistent with the measured data.

Thermal History Interpretation of (U-Th)/He Ages

Experimental investigations in recent years have led to a detailed understanding of the diffusion systematics of helium in apatite (e.g., Farley, 2000). This research, focused on the much-studied Durango apatite, suggests that diffusion systematics are controlled by physical grain size. This key observation implies that for any specified thermal history, (U-Th)/He ages can be modeled for a particular sample using the mean grain size and empirical estimates of the key diffusion parameters E_a (33 ± 0.5 kcal/mol) and log (D_o) (1.5 ± 0.6 cm^2/s). These values have been used in modeling (U-Th)/He ages for our study.

Because of the greater diffusive loss from smaller grains compared to larger grains, grain size differences may be significant in the interpretation of apatites from sedimentary rocks that have been heated to paleotemperatures within the helium partial retention zone. In such cases, grains of different radii give different ages for a given thermal history (Reiners and Farley, 2001). Therefore, incorporation of grain size effects into the modeling is essential, and grain sizes have been measured in all samples analyzed for our study (Table 4).

Modeling of Fresne-1 Helium Data

To more fully understand the Helium age results shown in Figure 9, we have modeled the values expected in each sample on the basis of the thermal history framework obtained from the AFTA and R_o data (Figure 8a). This has been carried out using software provided by Ken Farley of the California Institute of

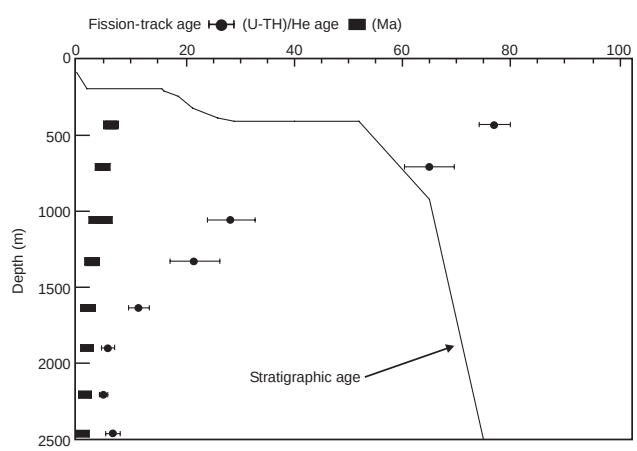

Figure 9. (U-Th)/He and fission-track ages measured in apatite grains from the Fresne-1 well plotted vs. depth. The variation of stratigraphic age with depth through the section is also shown, for comparison.

Technology, based on the systematics presented in Farley (2000).

Figure 10a shows (U-Th)/He ages predicted by the thermal histories shown in Figure 8a for four grain radii. Based on the mean radii in the samples analyzed from well Fresne-1 (Table 4), the trend for 50 μm radius grains is the most appropriate for direct comparison with the measured ages (Figure 10). In general, the predicted and measured ages in Figure 10a show a fair degree of agreement, particularly at the shallowest and deepest extremes of the depth range, whereas predicted values from the middle of the sampled interval are higher than measured values.

Given that predictions are based purely on diffusion systematics derived from extrapolation of results under laboratory conditions, it is not clear whether the slight mismatch between measured and predicted ages in Figure 10a arises because of differences in thermal history from those in Figure 8a or because of slight errors in the diffusion systematics. Comparison of

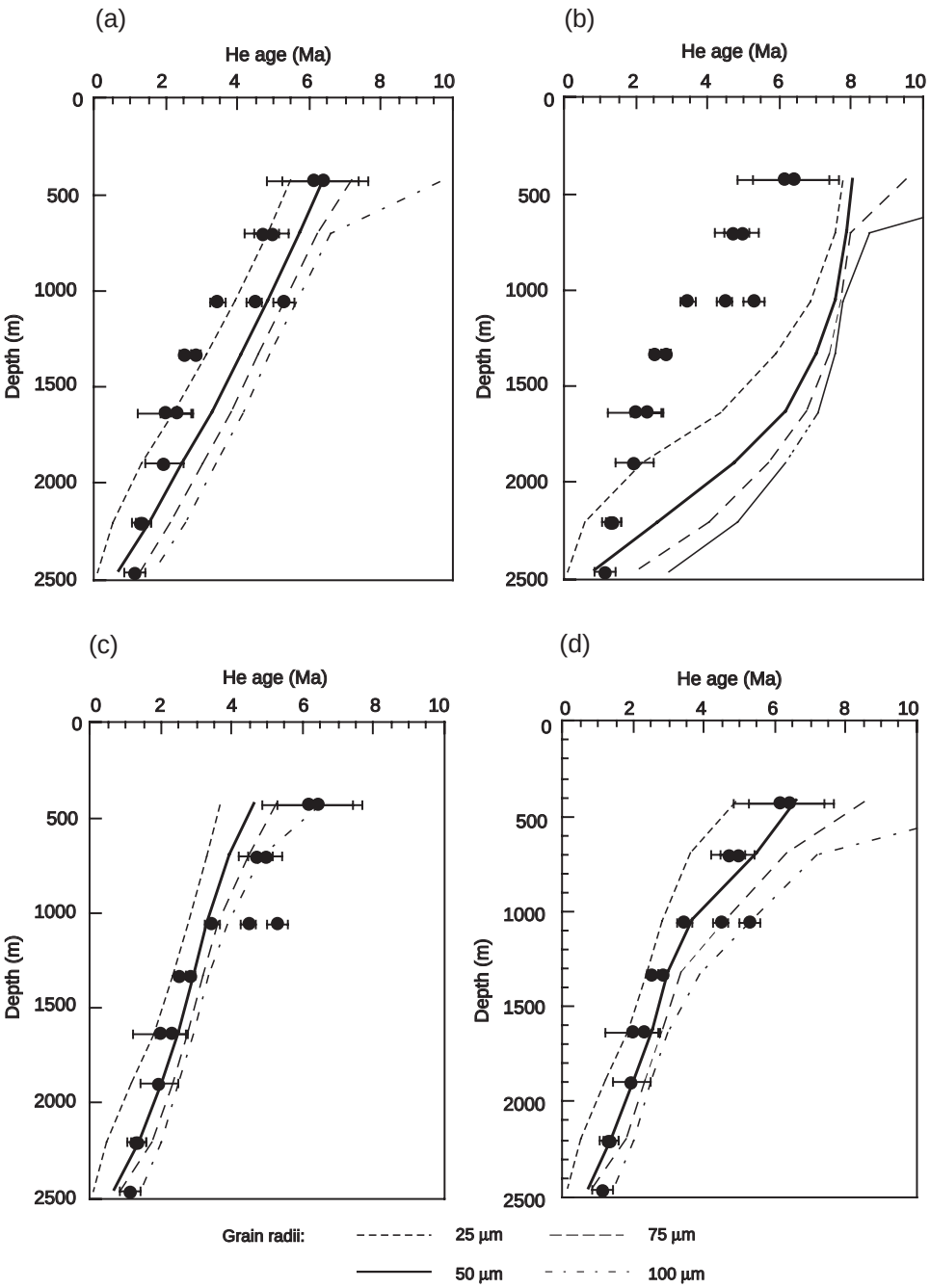

Figure 10. Variation of apatite (U-Th)/He age with depth predicted by the four thermal history scenarios illustrated in Figure 8 compared with measured apatite (U-Th)/He ages: (a) linear heating and cooling; (b) rapid cooling; (c) protracted cooling; (d) two separate cooling events. Scenario (d), involving two discrete cooling episodes, provides the best fit to the measured ages, but this is difficult to reconcile with the basin stratigraphy and structure, and on this basis scenario (c), involving protracted cooling, is considered more likely. Modeling predictions are based on helium diffusion systematics reported by Farley (2000).

measured (U-Th)/He ages with predicted values in samples from wells in the Otway Basin of southeastern Australia by House et al. (1999) suggest that the diffusion systematics can be extrapolated to geological conditions with confidence. On this basis, we have investigated how the thermal histories in Figure 8a might be refined to give a better fit to the measured ages.

Figure 8b shows an alternative thermal history style, characterized by rapid cooling from the maximum at 8.5 Ma and all cooling achieved within 1 m.y. This scenario predicts much older ages than for the slower cooling case (Figure 10b) and a much worse fit to the measured ages. Figure 8c illustrates a scenario involving protracted cooling, involving cooling by 25°C between 8.5 and 4 Ma and the remaining 50°C cooling between 4 and 2 Ma. The predicted age trends (Figure 10c) show an improved match to the measured ages, especially at depths greater than about 1000 m, but the predicted ages in the two shallowest samples are younger than the measured values, indicating that these samples cooled earlier than the deeper samples. This could suggest a thermal history scenario involving two discrete cooling episodes (Figure 8d), with an initial phase at 8.5 Ma and a later cooling phase beginning at 4 Ma (with 50°C of cooling since 4 Ma). In this case, the agreement between measured and predicted ages is extremely good through the whole depth range (Figure 10d).

At present, it is not clear whether this treatment represents overreliance on the extrapolation of laboratory diffusion systematics, and more tests are required in controlled geological conditions. However, these results illustrate the potential of the (U-Th)/He technique to complement AFTA and R_o data in sedimentary basins and to provide further definition of thermal histories, particularly in relation to more recent low-temperature events.

DISCUSSION

A scenario involving two discrete cooling episodes clearly provides a superior fit to the measured (U-Th)/He ages compared to a protracted cooling scenario. Such a history would be highly consistent with the chronology of uplift across the modern plate boundary in South Island, to the south of the Taranaki Basin. Thermochronological data from the southern Alps reveal clear evidence for two main pulses of uplift and erosion to the east of the Alpine fault (e.g., White and Green, 1986; Kamp et al., 1989), with an initial phase at around 10 to 9 Ma and the main episode of exhumation beginning at around 6 to 4 Ma.

However, because the accuracy of predicted (U-Th)/He age trends in geological conditions has yet to be rigorously evaluated, it may be premature to place too literal an interpretation on the modeling results discussed in the preceding section. The structural and stratigraphic development of the southern parts of the Taranaki Basin, and in particular the Wakamarama Anticline, provides no direct evidence to support the notion of two separate late Neogene cooling events in that area, if the thermal events were driven by cycles of burial and subsequent exhumation (i.e., inversion). Because a history involving protracted cooling (Figures 8c, 10c) gives an acceptable solution to both the basin stratigraphy and structure and the integrated thermochronological data, we consider this a more likely scenario at this stage.

The particular value in our study of integrating (U-Th)/He thermochronometry with thermal history reconstruction based on AFTA and R_o lies in better definition of the overall style (and to some extent the rate) of cooling following the late Miocene paleotemperature maximum. Because of the degree of heating and cooling (burial and exhumation) involved, all samples reached maximum paleotemperatures sufficient to totally reset the (U-Th)/He ages and did not begin to retain helium until they cooled to much lower temperatures, well after the initiation of late Miocene cooling. For this reason, the (U-Th)/He ages do not record the timing of initiation of cooling, which is recorded by the fission-track parameters for particular samples in the well section. However, AFTA is not as sensitive as the (U-Th)/He thermochronometer in apatite to temperatures below 70°C, and, therefore, the (U-Th)/He ages can be used to control the nature of the cooling history. In addition, modeling of the (U-Th)/He ages helps confirm the 2 Ma timing of cessation of cooling in the Fresne-1 well and the very rapid change from uplift and erosion to renewed basin subsidence and sedimentation over the site of Fresne-1. In summary, our study shows that a more complete reconstruction of the thermal history of the well section is possible by integration of multiple thermochronometers than by application of any one technique alone.

The interval of inversion and erosion at the Fresne-1 well between 8.5 and 2 Ma coincides with the timing of widespread compression in northwestern South Island (White and Green, 1986; Kamp et al., 1992; Kamp et al., 1996, Kamp et al., 1999), which started at about 10 Ma and is ongoing. The geodynamic cause

of this shortening is the development of an obliquely convergent continent-continent collision zone in South Island. The inversion structures in the Taranaki Basin represent the distal northern expression of the crustal shortening more strongly developed on land to the south. The late and sudden transition in the Fresne-1 well from cooling (exhumation) to heating (burial) at about 2 Ma coincides with the passage of the leading edge of the subducted slab of the Pacific plate beneath the vicinity of the well site (Kamp, 1999; Kamp and Xu, 2002).

IMPLICATIONS FOR HYDROCARBON EXPLORATION

Aside from high-level stratigraphic traps in upper Miocene sequences in the Taranaki Peninsula, all the known condensate and oil fields in the Taranaki Basin are present in structural traps. Positive inversion structures in the southern part of the basin provide traps for three oil and gas fields (Maui, Kapuni, and Kupe South), as well as several other fields (Toru, Moki) (King and Thrasher, 1996). A critical element in assessing particular prospects is the timing of maximum temperatures, and the consequent expulsion of oil and gas, in relation to the timing of structure (trap) formation. Armstrong et al. (1996) undertook comprehensive modeling of the thermal and hydrocarbon generation history of the succession encountered in the Fresne-1 well and other well sections in the basin. Because of the rapid deposition of thick (>4000 m) Upper Cretaceous deposits (Rakopi Formation, Pakawau Group), oil generation and expulsion at the level of the top of basement in the Fresne-1 well began about 70 Ma. The Wakamarama Anticline was clearly not a potential trap for this phase of hydrocarbon generation and expulsion. Subsequently, maximum temperatures at all horizons declined by about 20°C during the late rift-drift phase of basin evolution (Armstrong et al., 1996). During the middle–late Miocene, maximum temperatures increased by about 70°C and the Pakawau Group reentered the oil generation and expulsion window. This phase of generation and expulsion also predated the age of formation of the potential trap (Wakamarama Anticline), which occurred during the late Miocene–Pliocene. As a result, the hydrocarbons generated during this phase would have migrated elsewhere.

Although hydrocarbons from source beds low in the Wakamarama Anticline succession dispersed before the structure formed, they could have migrated into it from elsewhere in the basin after the onset of inversion. The accumulations in the Maui field, for example, are interpreted to have migrated there after the late Miocene inversion (Thrasher, 1989). In the central and northern parts of the Taranaki Basin, most potential source rocks (Pakawau and Kapuni groups) probably reached maturity for hydrocarbon expulsion during or following deep burial during the past 10 m.y. (Armstrong et al., 1996; King and Thrasher, 1996). Hence, (long distance) migration would need to have occurred for petroleum fluids to reach structures in the southern parts of the basin. In such situations, understanding and prediction of present-day hydrocarbon accumulations in the region requires precise estimation of the chronology of inversion and its variation across the region. With protracted cooling (perhaps involving two discrete inversion phases) clearly indicated by the integrated AFTA and (U-Th)/He data, the possibility exists that hydrocarbons may have undergone repeated cycles of migration. The modification of structural traps by progressive (or separate phases of) inversion must also be considered.

Our study shows that better constraints can be established on the timing and duration of structure (trap) formation by integrated application and modeling of low-temperature thermochronological methods such as AFTA and (U-Th)/He dating. The application of these techniques to more structures in the Taranaki Basin (and similar approaches in other prospective basins) will provide improved resolution in the chronology of inversion and has the potential to significantly reduce exploration risk by focusing on more prospective areas where the final phase of hydrocarbon migration postdated formation of structures.

APPENDIX: (U-TH) /HE DATING: ANALYTICAL PROCEDURES

The helium extraction and analysis facility used in our study comprises an all-metal helium extraction and gas-handling line connected to a dedicated on-line Balzers Prisma 200 quadrupole mass spectrometer. Gas extraction was performed using a vacuum resistance furnace, where samples are heated to about 900°C for about 15 minutes. The line and furnace are evacuated via ion, turbo, and backing pumps. Active gases, particularly hydrogen, are removed using SAES getters. The analysis procedure is operated by LabVIEW automation software supplied by Ken Farley of the California Institute of Technology.

Apatite grains are carefully handpicked to avoid U- and Th-rich mineral inclusions that may produce excess helium (e.g., zircon). Images of selected grains are captured by a closed-circuit digital video

camera mounted on the microscope and measured using image analysis techniques for the purposes of an alpha ejection correction calculation (Farley et al., 1996). Aliquots of approximately 5–30 similar size grains (radius typically >40 and <150 μm) are sealed into stainless steel capsules and are heated to about 900°C for about 15 minutes.

Abundances of ^{4}He are determined by isotope dilution using a pure ^{3}He spike, which is calibrated on a regular basis against an independent ^{4}He standard. Hot blanks of ^{4}He (or reextracts) are performed routinely before and after each sample. The U and Th content of degassed apatite samples are determined on a Perkin Elmer Sciex 5000a inductively coupled plasma mass spectrometer using the isotope ratio application. We added 100 μl of each ^{235}U and ^{230}Th spike solution (about 5 and 6 ng, U and Th, respectively) and 200 μl of concentrated nitric acid to a vial containing the capsule and degassed apatite. The 100 μl of 0.25 ppm U and Th standard solutions (Johnson Matthey) are similarly spiked and acidified. We have determined the ^{235}U/^{238}U ratio of the Johnson Matthey U-standard solution to be 135, close to the natural value of 138.

Helium diffusion rates in apatite are related to grain radius (Farley, 2000). Because the closure temperature varies with grain size it becomes an important parameter in modeling the expected patterns of helium age for a specified thermal history. The overall variation in closure temperature for samples with grain radii of 50–150 μm is only 5°C. This difference may be significant in the interpretation of apatites from drill holes that have resided within the partial retention zone for prolonged periods of time (House et al., 2002). In general, aliquots composed of larger grains are expected to yield an older age than aliquots of the same sample that consist of smaller grains, especially in the case of slow cooling (Farley, 2000; House et al., 2002).

Wolf et al. (1996) and House et al. (2002) suggested that the composition of the apatite does not appear to affect the sensitivity of the helium closure temperature, which is in contrast to the effect chlorine content has on AFTA annealing kinetics.

REFERENCES CITED

Armstrong, P. A., D. S. Chapman, R. N. Funnell, R. G. Allis, and P. J. J. Kamp, 1996, Thermal modelling and hydrocarbon generation in an active-margin basin: the Taranaki Basin: AAPG Bulletin, v. 80, p. 1216–1241.

Armstrong, P. A., R. G. Allis, R. N. Funnell, and D. S. Chapman, 1998, Late Neogene exhumation patterns in Taranaki Basin (New Zealand): evidence from offset porosity-depth trends: Journal of Geophysical Research, v. 103, p. 30,269–30,282.

Bishop, D. J., and P. G. Buchanan, 1995, Development of structurally inverted basins: a case study from the West Coast, South Island, New Zealand, *in* D. G. Buchanan and P. G. Buchanan, eds., Basin inversion: Geological Society Special Publication 88, p. 549–585.

Bray, R., P. F. Green, and I. R. Duddy, 1992, Thermal history reconstruction in sedimentary basins using apatite fission track analysis and vitrinite reflectance: a case study from the east Midlands of England and the southern North Sea, *in* R. F. P. Hardman, ed., Exploration Britain: into the next decade: Geological Society Special Publication 67, p. 3–25.

Burnham, A. K., and J. J. Sweeney, 1989, A chemical kinetic model of vitrinite reflectance maturation: Geochimica et Cosmochimica Acta, v. 53, p. 2649–2657.

Duddy, I. R., P. F. Green, and G. M. Laslett, 1988, Thermal annealing of fission tracks in apatite 3: variable temperature behaviour: Chemical Geology, v. 73, p. 25–38.

Duddy, I. R., P. F. Green, K. A. Hegarty, and R. J. Bray, 1991, Reconstruction of thermal history in basin modelling using apatite fission track analysis: what is really possible: Proceedings of the First Offshore Australia Conference, p. III-49–III-61.

Duddy, I. R., P. F. Green, R. J. Bray, and K. A. Hegarty, 1994, Recognition of the thermal effects of fluid flow in sedimentary basins, *in* J. Parnell, ed., Geofluids: origin, migration and evolution of fluids in sedimentary basins: Geological Society Special Publication 78, p. 325–345.

Ellyard, T., and B. Beattie, 1990, Inversion structures and hydrocarbon potential of the southern Taranaki Basin, *in* 1989 New Zealand Oil Exploration Conference Proceedings: Wellington, New Zealand, Ministry of Commerce, p. 259–271.

Farley, K. A., 2000, Helium diffusion from apatite: general behaviour as illustrated by Durango fluorapatite: Journal of Geophysical Research, v. 105, no. B2, p. 2903–2914.

Farley, K. A., R. A. Wolf, and L. T. Silver, 1996, The effects of long alpha-stopping distances on (U-Th)/He ages: Geochimica et Cosmochimica Acta, v. 60, p. 4223–4229.

Funnell, R. H., D. S. Chapman, R. G. Allis, and P. A. Armstrong, 1996, Thermal state of the Taranaki Basin, New Zealand: Journal of Geophysical Research, v. 101, p. 25,197–25,515.

Galbraith, R. F., and G. M. Laslett, 1993, Statistical methods for mixed fission track ages: Nuclear Tracks, v. 21, p. 459–470.

Green, P. F., 1985, Comparison of zeta calibration baselines for fission-track dating of apatite, zircon and sphene: Chemical Geology, v. 58, p. 1–22.

Green, P. F., I. R. Duddy, A. J. W. Gleadow, P. R. Tingate, and G. M. Laslett, 1986, Thermal annealing of fission tracks in apatite 1: a qualitative description: Chemical Geology, v. 59, p. 237–253.

Green, P. F., I. R. Duddy, G. M. Laslett, K. A. Hegarty, A. J. W. Gleadow, and J. F. Lovering, 1989, Thermal annealing of fission tracks in apatite 4: quantitative modelling techniques and extension to geological timescales: Chemical Geology, v. 79, p. 155–182.

Green, P. F., I. R. Duddy, and J. R. Bray, 1995, Applications of thermal history reconstruction in inverted basins, *in* J. G. Buchanan and P. G. Buchanan, eds., Basin inversion: Geological Society Special Publication 88, p. 149–165.

Green, P. F., K. A. Hegarty, and I. R. Duddy, 1996, Compositional influences on fission track annealing in apatite and improvement in routine application of AFTA (abs.): AAPG Annual Convention, Abstracts with Program, v. 5, p. A56.

Green, P. F., I. R. Duddy, and K. A. Hegarty, in press, Quantifying exhumation in sedimentary basins of the UK from apatite fission track analysis and vitrinite reflectance data: precision, accuracy and latest results, *in* A. G. Dore, J. A. Cartwright, M. S. Stoker, J. P. Turner, and N. J. White, eds., Exhumation of the circum-Atlantic margins: Geological Society Special Publication.

House, M. A., B. P. Wernicke, K. A. Farley, and T. A. Dumitru, 1997, Cenozoic thermal evolution of the central Sierra Nevada, California, from (U-Th)/He thermochronometry: Earth and Planetary Science Letters, v. 151, p. 167–179.

House, M. A., K. A. Farley, and B. P. Kohn, 1999, An empirical test of helium diffusion in apatite: borehole data from the Otway Basin, Australia: Earth and Planetary Science Letters, v. 170, p. 463–474.

House, M. A., B. P. Kohn, K. A. Farley, and A. Raza, 2002, Evaluating thermal history models for the Otway Basin, southeastern Australia, using (U-Th)/He and fission-track data from borehole apatites: Tectonophysics, v. 349, p. 277–295.

Hurford, A. J. H., and P. F. Green, 1983, The zeta age calibration

of fission-track dating: Chemical Geology, v. 41, no. 4, p. 285–317.

Kamp, P. J. J., 1999, Tracking crustal processes by FT thermochronology in a fore-arc high (Hikurangi margin, New Zealand) involving Cretaceous subduction termination and mid-Cenozoic subduction initiation: Tectonophysics, v. 307, p. 313–343.

Kamp, P. J. J., and P. F. Green, 1990, Thermal and tectonic history of selected Taranaki Basin (New Zealand) wells assessed by apatite fission track analysis: AAPG Bulletin, v. 74, p. 1401–1419.

Kamp, P. J. J., and G. Xu, 2002, Thermal history of Opoutama-1, Hawke's Bay Basin: implications for hydrocarbon prospectivity, *in* Proceedings of the New Zealand Oil Conference: Wellington, New Zealand, Ministry of Economic Development.

Kamp, P. J. J., P. F. Green, and S. J. White, 1989. Fission track analysis reveals character of collisional tectonics in New Zealand: Tectonics, v. 8, p. 169–195.

Kamp, P. J. J., P. F. Green, and J. M. Tippett, 1992, Tectonic architecture of the mountain front–foreland basin transition, South Island, New Zealand, assessed by fission track analysis: Tectonics, v. 8, p. 169–195.

Kamp, P. J. J., K. S. Webster, and S. Nathan, 1996, Thermal history analysis by integrated modelling of apatite fission track and vitrinite reflectance data: application to an inverted basin (Buller coalfield, New Zealand): Basin Research, v. 8, p. 383–402.

Kamp, P. J. J., I. W. S. Whitehouse, and J. Newman, 1999, Constraints on the thermal and tectonic evolution of the Greymouth coalfield, New Zealand: New Zealand Journal of Geology and Geophysics, v. 43, p. 447–467.

King, P. R., and G. P. Thrasher, 1996, Cretaceous–Cenozoic geology and petroleum systems of the Taranaki Basin, New Zealand: Institute of Geological and Nuclear Sciences Monograph 13, 243 p.

King, P. R., T. R. Naish, and G. P. Thrasher, 1991, Structural cross-sections and selected palinspastic reconstructions of the Taranaki Basin, New Zealand: New Zealand Geological Survey Report G150, unpaginated.

Knox, G. J., 1982, Taranaki Basin, structural style and tectonic setting: New Zealand Journal of Geology and Geophysics, v. 25, p. 125–140.

Laslett, G. M., P. F. Green, I. R. Duddy, and A. J. W. Gleadow, 1987, Thermal annealing of fission tracks in apatite 2: a quantitative analysis: Chemical Geology, v. 65, p. 1–13.

Lippolt, H. J., M. Leitz, R. S. Wernicke, and B. Hagedorn, 1994, (Uranium + thorium)/helium dating of apatite: experience with samples from different geochemical environments: Chemical Geology, v. 112, p. 179–191.

Lowery, J. H., 1988, Catalogue of vitrinite reflectance measurements and coal analyses from oil prospecting wells in Taranaki Basin, New Zealand: New Zealand Geological Survey Report M168, 50 p.

Reiners, P. W., and K. A. Farley, 2001, Influence of crystal size on apatite (U-Th)/He thermochronology: an example from the Bighorn Mountains, Wyoming: Earth and Planetary Science Letters, v. 188, p. 413–420.

Rutherford, E., 1907a, Die Radioaktivität: Berlin, Springer, 595 p.

Rutherford, E., 1907b, Radioaktive Umwandlungen (Silliman—Vorlesungen 1905): Braunschwieg, Vieweg, 285 p.

Sweeney, J. J., and A. K. Burnham, 1990, Evaluation of a simple model of vitrinite reflectance based on chemical kinetics: AAPG Bulletin, v. 74, p. 1559–1570.

Thrasher, G. P., 1989, Tectonics of the Taranaki Rift, *in* 1989 New Zealand Oil Exploration Conference Proceedings: Wellington, New Zealand, Ministry of Commerce, p. 124–133.

Warnock, A. C., P. K. Zeitler, R. A. Wolf, and S. C. Bergman, 1997, An evaluation of low-temperature apatite U-Th/He thermochronometry: Geochimica et Cosmochimica Acta, v. 61, p. 5371–5377.

White, S. H., and P. F. Green, 1986, Tectonic development of the Alpine fault zone, New Zealand: a fission track study: Geology, v. 14, p. 124–127.

Wolf, R. A., K. A. Farley, and L. T. Silver, 1996, Helium diffusion and low-temperature thermochronometry of apatite: Geochimica et Cosmochimica Acta, v. 60, p. 4231–4240.

Wolf, R. A., K. A. Farley, and L. T. Silver, 1997, Assessment of (U-Th)/He thermochronometry: the low temperature history of the San Jacinto mountains, California: Geology, v. 25, p. 65–68.

Wolf, R. A., K. A. Farley, and D. M. Wolf, 1998, Modelling of the temperature sensitivity of the apatite (U-Th)/He thermochronometer: Chemical Geology, v. 148, p. 105–114.

Zeitler, P. K., A. L. Herczig, I. McDougall, and M. Honda, 1987, U-Th-He dating of apatite: a potential thermochronometer: Geochimica et Cosmochimica Acta, v. 51, p. 2865–2868.